Spin-Lattice and Magnetoelectric Couplings Enhanced by Orbital Degrees of Freedom in Polar Multiferroic Semiconductors

Vilmos Kocsis,[1,2] Yusuke Tokunaga,[1,3] Toomas Rõõm,[4] Urmas Nagel,[4] Jun Fujioka,[5] Yasujiro Taguchi,[1] Yoshinori Tokura,[1,6] and Sándor Bordács[7,8]

[1]*RIKEN Center for Emergent Matter Science (CEMS), Wako, Saitama 351-0198, Japan*
[2]*Institut für Festkörperforschung, Leibniz IFW-Dresden, 01069 Dresden, Germany*
[3]*Department of Advanced Materials Science, University of Tokyo, Kashiwa 277-8561, Japan*
[4]*National Institute of Chemical Physics and Biophysics, 12618 Tallinn, Estonia*
[5]*Institute of Materials Science, University of Tsukuba, Ibaraki 305-8573, Japan*
[6]*Tokyo College and Department of Applied Physics, University of Tokyo, Hongo, Tokyo 113-8656, Japan*
[7]*Department of Physics, Institute of Physics, Budapest University of Technology and Economics, Műegyetem rkp. 3, H-1111 Budapest, Hungary*
[8]*Quantum Phase Electronics Center and Department of Applied Physics, University of Tokyo, Tokyo 113-8656, Japan*

(Received 21 August 2022; accepted 7 December 2022; published 18 January 2023)

Orbital degrees of freedom mediating an interaction between spin and lattice were predicted to raise strong magnetoelectric effect, i.e., to realize an efficient coupling between magnetic and ferroelectric orders. However, the effect of orbital fluctuations has been considered only in a few magnetoelectric materials, as orbital-degeneracy driven Jahn-Teller effect rarely couples to polarization. Here, we explore the spin-lattice coupling in multiferroic Swedenborgites with mixed valence and Jahn-Teller active transition metal ions on a stacked triangular and Kagome lattice using infrared and dielectric spectroscopy. On one hand, in $CaBaM_4O_7$ (M = Co, Fe), we observe a strong magnetic-order-induced shift in the phonon frequencies and a corresponding large change in the dielectric response. Remarkably, as an unusual manifestation of the spin-phonon coupling, the spin fluctuations reduce the phonon lifetime by one order of magnitude at the magnetic phase transitions. On the other hand, lattice vibrations, dielectric response, and electric polarization show no variation at the Néel temperature of $CaBaFe_2Co_2O_7$, which is built up by orbital singlet ions. Our results provide a showcase for orbital degrees of freedom enhanced magnetoelectric coupling via the example of Swedenborgites.

DOI: 10.1103/PhysRevLett.130.036801

Spin-orbit coupling (SOC) is considered among the most essential interactions in condensed matter science, standing in the background of topological insulators [1] and superconductors [2], Dirac and Weyl semimetals [3,4], Kitaev physics [5], as well as multiferroics [6,7]. In the latter compounds, SOC induces magnetoelectric (ME) coupling between electric polarization and magnetism making them interesting for basic research and appealing for applications; however, this interaction is usually weak due to its relativistic nature [8–12]. While the relativistic spin-orbit interaction enables the ME coupling on a single (a pair) of magnetic ion(s), theoretical works proposed early that the charge and orbital degrees of freedoms can mediate an enhanced ME interaction via the Kugel-Khomskiĭ-type spin-orbital coupling [13–16]. However, materials realizing this scenario are exceptional, as charge and orbital order alone rarely break the inversion symmetry [16–22]. The two most studied cases are Fe_3O_4, where the ME effect is attributed to the charge and orbital orderings [16–19], and $LuFe_2O_4$ in which the ferroelectricity is debated to emerge from charge ordering [20]. Recently, $CaMn_7O_{12}$ was also identified with a chiral magnetic structure stabilized by the charge and orbital ordering [21,22].

Swedenborgites $CaBaM_4O_7$ (M = Co, Fe) provide another platform to study the interplay between spins and orbitals, but there, unlike the previous examples, the charge degree of freedom is quenched. The polar Swedenborgites are built up by alternating layers of triangular and kagomé sheets of MO_4 tetrahedra, all pointing to the c axis, as shown in Fig. 1(a). The $M^{2.5+}$ nominal valence suggests a 1:1 mixture of M^{2+} and M^{3+} ions, subjected to geometric frustration. The buckling of the kagomé lattice releases the frustration and reduces the symmetry to orthorhombic at $T_S = 450$ K [23,24] and $T_S = 380$ K [27,28] in $CaBaCo_4O_7$ and $CaBaFe_4O_7$, respectively. In both compounds, x-ray spectroscopy studies confirmed the coexistence of distinct valences, M^{2+} and M^{3+} (electron configurations sketched in Fig. 2), and suggested charge order with the M^{3+} ions occupying the triangular and one of the kagomé sites [23,27,29–31]. Therefore, both $CaBaCo_4O_7$ and $CaBaFe_4O_7$ contain the Jahn-Teller active Co^{3+} and Fe^{2+} ions, respectively, though, no further information is

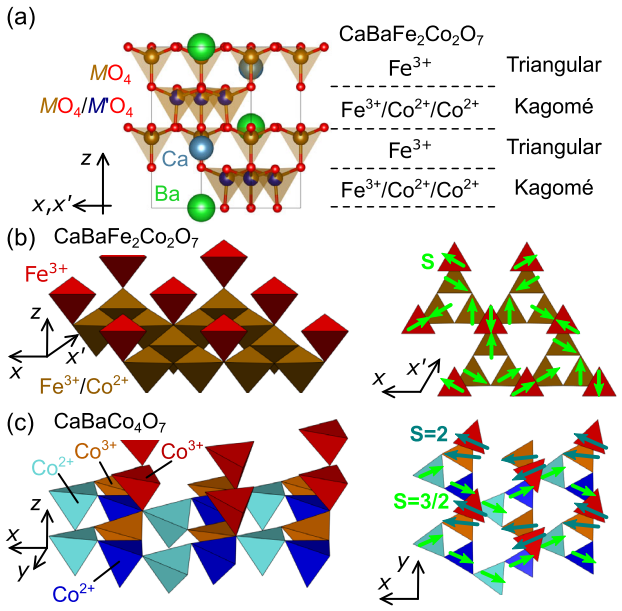

FIG. 1. (a) The polar structural unit cell of trigonal Swedenborgites are built up by alternating triangular and Kagomé layers of coaligned MO_4 tetrahedra. (b) In the trigonal $CaBaFe_2Co_2O_7$, one Fe^{3+} ion occupies the triangular lattice, while the remaining $Fe^{3+}/Co^{2+}/Co^{2+}$ ions are distributed randomly on the Kagome lattice. The $\sqrt{3}\times\sqrt{3}$-type antiferromagnetic order develops below $T_N = 152$ K (spin **S**, green arrow, reproduced after Ref. [39].) (c) The orthorhombic $CaBaCo_4O_7$ has charge order and a ferrimagnetic order below $T_C = 60$ K, reproduced after Refs. [23,29].

available on orbital ordering. However, the solid solution $CaBaFe_2Co_2O_7$ lacks orbital degeneracy, namely solely the orbital singlet Fe^{3+} and Co^{2+} charge states are present in this compound [30–32].

In $CaBaCo_4O_7$, spins order antiferromegnetically at $T_N = 70$ K [33], and then a ferrimagnetic structure emerges below $T_C = 60$ K [23,34], as shown in Fig. 1(c). The latter phase is accompanied by one of the largest magnetic-order-induced polarizations detected so far [35,36] as well as exceptionally large magnetostriction [37]. Its sister compound, $CaBaFe_4O_7$ also shows peculiar ME properties. It becomes multiferroic close to room temperature, $T_{C1} = 275$ K upon a ferrimagnetic ordering, which is followed by a reorientation transition below $T_{C2} = 211$ K [27,28]. $CaBaFe_2Co_2O_7$ develops an antiferromagnetic structure at $T_N = 152$ K [32,38,39] [Fig. 1(b)]; however, its ME properties have been unknown.

In this Letter, we investigate the effect of magnetic ordering on the charge dynamics of Swedenborgites via infrared and dielectric spectroscopy. We compared members of the material family with and without orbital degree of freedom, and found a strong spin-lattice coupling only in $CaBaM_4O_7$ (M = Co, Fe) with Jahn-Teller active ions. In these pristine compounds, the phonon frequencies show a sudden shift at T_C, related to the large magnetic-order-induced polarization and magnetocapacitance. Moreover, we observed one order of magnitude decrease of the phonon lifetimes at the ferrimagnetic phase transitions. In contrast, we found no phonon or dielectric anomalies and negligible change in the pyroelectric polarization upon the magnetic ordering in the orbital singlet $CaBaCo_2Fe_2O_7$. Therefore, our results highlight the importance of orbital degrees of freedom in the enhancement of the spin-lattice interaction and the ME effect in multiferroics.

Large single crystals of $CaBaCo_4O_7$, $CaBaFe_4O_7$, $CaBaFe_2Co_2O_7$, and $YBaCo_3AlO_7$ were grown by the floating zone technique [28,32,35,40,41]. Polarized, near normal incidence reflectivity was measured on polished cuts. Temperature dependent experiments were carried out up to 40 000 cm^{-1} with an FT-IR spectrometer (Vertex80v, Bruker) and a grating-monochromator spectrometer (MSV-370YK, Jasco). The reflectivity spectrum of each compound was measured up to 250 000 cm^{-1} at room temperature with the use of synchrotron radiation at UVSOR Institute for Molecular Science, Okazaki, Japan. The optical conductivity was calculated using the Kramers-Kronig transformation [24]. The pyroelectric polarization was obtained by measuring and integrating the displacement current with an electrometer (6517A, Keithley) while the temperature was swept in a Physical Property Measurement System (PPMS, Quantum Design). The dielectric properties were also measured in a PPMS, using an LCR meter (E4980A, Keysight Technologies) while the ac magnetization was measured in a Magnetic Property Measurement System (Quantum Design).

For quantitative analysis, we fitted the real part of the optical conductivity as a sum of Lorentz oscillators:

$$\sigma(\omega) = -i\omega\epsilon_0\left[\epsilon_\infty + \sum_j \frac{S_j}{\omega_{0,j}^2 - \omega^2 - i\gamma_j\omega}\right], \quad (1)$$

where $\omega_{0,j}$, S_j, and γ_j are the frequency, oscillator strength, and damping rate of the jth mode, and ϵ_∞ is the high-frequency dielectric constant, respectively.

In Fig. 2, we show the temperature dependence of the reflectivity and optical conductivity spectra around the lowest energy phonon modes of $CaBaCo_4O_7$, $CaBaFe_2Co_2O_7$, and $CaBaFe_4O_7$ for light polarization $\mathbf{E}^\omega \| z$. The reflectivity spectra over the whole photon energy range covered by our experiment for both $\mathbf{E}^\omega \| z$ and $\mathbf{E}^\omega \perp z$ are presented in the Supplemental Material [24]. The phonon spectra of $CaBaCo_4O_7$ and $CaBaFe_4O_7$ [see Figs. 2(a), 2(d), and, in the Supplemental Material, S3 [24], and Figs. 2(c) and 2(f), and, in the Supplemental Material, S4 [24], respectively) change markedly with temperature. The resonances are narrow at low temperatures and get significantly broader above the magnetic-ordering temperature. Contrary to the pristine compounds, the phonon modes of $CaBaFe_2Co_2O_7$ depend weakly on the

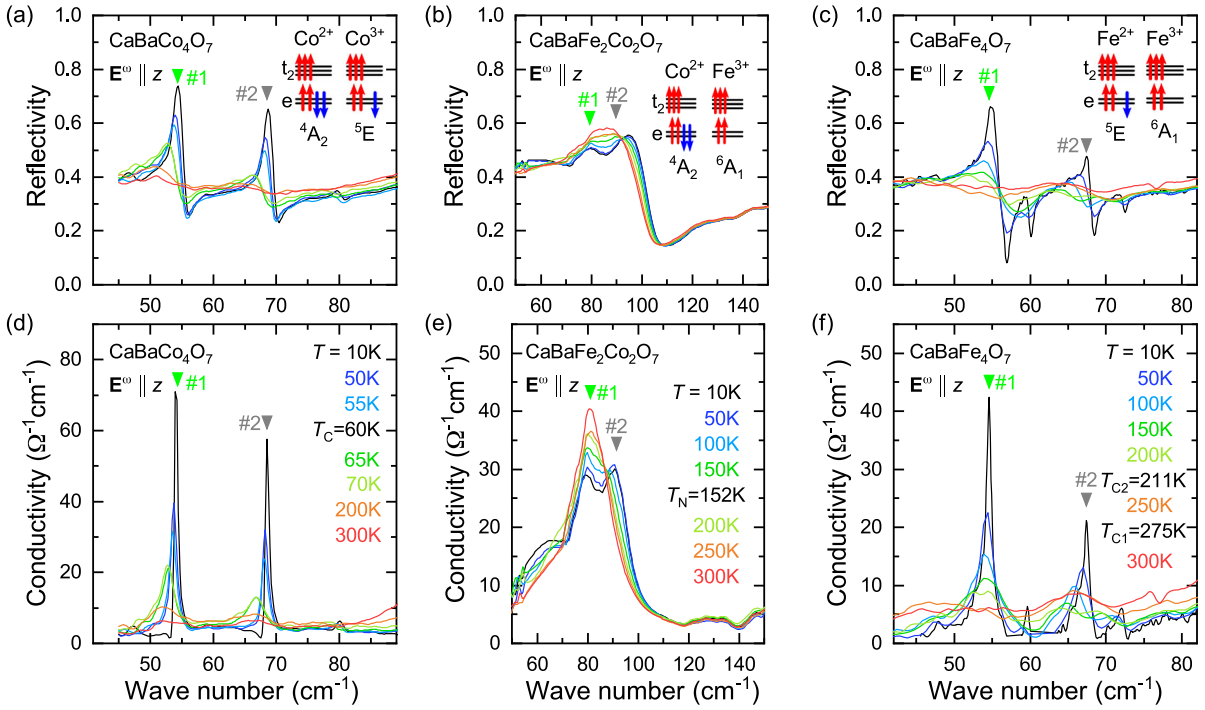

FIG. 2. The reflectivity and the optical conductivity spectra of (a) and (d) $CaBaCo_4O_7$, (b) and (e) $CaBaFe_2Co_2O_7$, and (c) and (f) $CaBaFe_4O_7$ at selected temperatures in the frequency range of the lowest energy phonon modes.

temperature and show no anomaly at T_N, as shown in Figs. 2(b), 2(e), and, in the Supplemental Material, S5 [24].

In Fig. 3, we compare the temperature dependence of the phonon parameters, frequency ($\omega_{0,j}$), and damping rate (γ_j) in $CaBaCo_4O_7$ and $CaBaFe_2Co_2O_7$ for selected, well-separated phonon modes. In the orthorhombic $CaBaCo_4O_7$ and $CaBaFe_4O_7$, the phonon modes are nondegenerate already at room temperature, and we did not resolve new modes below the magnetic phase transition temperatures. However, in both compounds the phonon frequencies change abruptly at the onset of the ferrimagnetic phase transitions. As an example, the magnitude of phonon energy shift becomes as large as $\Delta\omega_0/\omega_0 \sim 4\%$ for modes 1 and 2 in $CaBaCo_4O_7$, shown in Fig. 3(a). This is significantly higher than $\Delta\omega_0/\omega_0 \sim 1\%$, the highest value observed in other multiferroics [42–44] and in magnets with strong spin-phonon coupling [45,46]. This indicates an extremely strong spin-lattice coupling [47–50], which agrees with recent experiments demonstrating giant magnetostriction [37]. In $CaBaFe_2Co_2O_7$, however, the phonon frequencies change slightly with the temperature, and we could not resolve any splitting of the phonon modes (see Figs. S5 and S8 in the Supplemental Material [24]).

The most remarkable changes in the infrared spectra of $CaBaCo_4O_7$ and $CaBaFe_4O_7$ are the drastic increase in the damping rates of all phonon modes as warmed above the ferrimagnetic phase transitions; see Fig. 3 and, in the Supplemental Material [24], S8, respectively. Modes 1 and 2 of $CaBaCo_4O_7$ well exemplify this tendency: At $T = 10$ K the damping rates of these modes are as low as 0.5 cm^{-1}. Such sharp phonons with $\gamma/\omega_0 < 1\%$ are unusual in condensed matter systems, and only observed in nonmagnetic molecular crystals [51–54]. However, in the vicinity of T_C the phonon lifetime decreases, i.e., the damping rate grows by 1 order of magnitude indicating a strong scattering of phonons by spin fluctuations. In the paramagnetic phase, γ keeps increasing, and at room temperature the phonon modes are strongly damped with γ/ω_0 ratios exceeding 10%. The strong temperature dependence of the damping rates away from T_C, besides the strong spin-lattice coupling, suggests strong lattice anharmonicity [55,56]. The damping rates of modes 16 and 21, and those of $CaBaFe_4O_7$ (see Fig. S8 in the Supplemental Material [24]) follow similar temperature dependence with pronounced change at the ferrimagnetic phase transitions. In contrast, the damping rates in $CaBaFe_2Co_2O_7$ show weak temperature dependence and no anomalies at T_N.

As demonstrated in Fig. 4 and, in the Supplemental Material [24], S9, the emergence of magnetic order strongly influences the pyroelectric polarization and the low-frequency dielectric response of $CaBaCo_4O_7$. We observed large magnetic-order-induced polarization change for $P\|z$ in agreement with former results [35,36] and negligible for $P\perp z$ [57]. The real part of the dielectric constants, both $\epsilon_{\perp z}$ and $\epsilon_{\|z}$, exhibit a steplike change when crossing T_C [see Figs. 4(d) and 4(f)], with similar magnitude to that of in $DyMn_2O_5$ showing a colossal

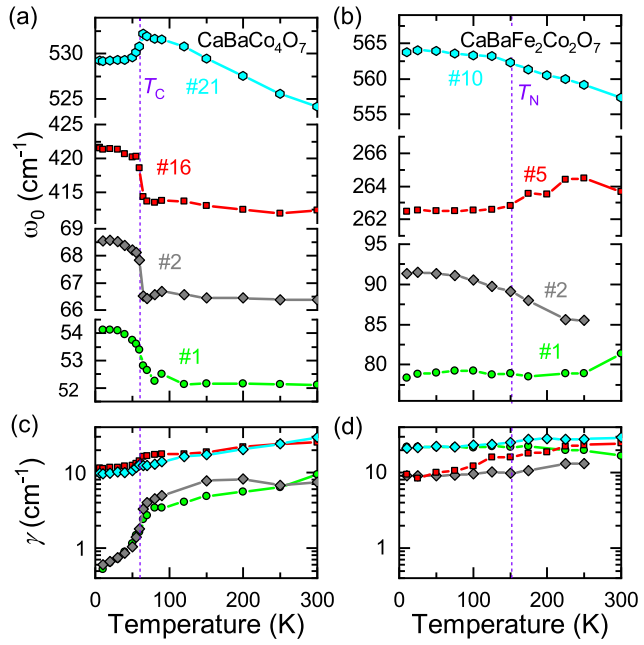

FIG. 3. (a) and (b) Temperature dependence of the fitted phonon frequencies (ω_0) and (c) and (d) damping rates (γ) in $CaBaCo_4O_7$ and $CaBaFe_2Co_2O_7$, respectively. The strong coupling between magnetic and elastic properties in $CaBaCo_4O_7$ is demonstrated by the changes in ω_0 and γ around the magnetic phase transition (T_C), indicated by dashed lines.

magnetodielectric effect [58]. Since the step height is independent of frequency between 10^2 and 10^5 Hz, and observed for both $\epsilon_{\perp z}$ and $\epsilon_{\parallel z}$, the drop in the static dielectric function is related to the sudden changes in the phonon resonances. In addition to the step edge in the real part, both the real and the imaginary parts of $\epsilon_{\parallel z}$ have a peak at the close vicinity of T_C. The frequency dependence and the related finite dissipation indicate electric dipoles with low-frequency dynamics and strong scattering. The peak shape in the real part suggests that the magnetic fluctuations can couple to electric dipoles and contribute to the phonon scattering [59,60]. Toward higher temperatures, the dielectric constants increase, not due to the change of phonon frequency but due to the decrease of the resistivity caused by the thermally activated carriers, as shown in Fig. S2 of the Supplemental Material [24]. Although $CaBaFe_2Co_2O_7$ has a similar pyroelectric crystal structure and a relatively high T_N, its polarization is not affected by the antiferromagnetic order, as displayed in Fig. 4(c). The dielectric properties of this compound show a smooth variation on temperature in accordance with the phonon spectrum.

We now discuss the enhanced scattering of phonons by spin fluctuations and the origin of the strong anomaly in the dielectric constant observed only in the pristine Swedenborgites, $CaBaCo_4O_7$ and $CaBaFe_4O_7$. Remarkably, such a large drop of the phonon damping rate induced by magnetic ordering is rare. Only minor changes in

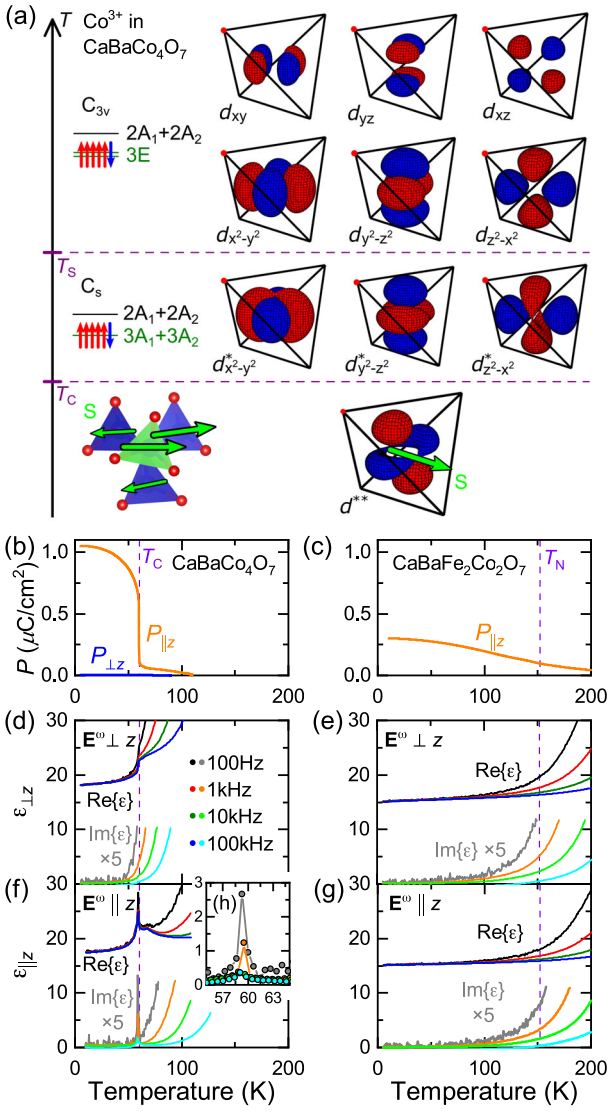

FIG. 4. (a) Schematics of the ground state multiplet structure of Jahn-Teller active Co^{3+} ion in $CaBaCo_4O_7$. The Jahn-Teller active Fe^{2+} ion in $CaBaFe_4O_7$ has the same multiplet structure. The magnetic ions in the tetrahedral environment (T_d) have the orbital-degenerate ^5E ground state, which is preserved by the spin-orbit interaction. At high temperature ($T_S < T$), the oxygen environment is distorted to the polar C_{3v} symmetry, but the orbital degeneracy is preserved by the E ground states $\{d_{x^2-y^2}, d_{xy}\}$. The trigonal to orthorombic distortion decreases the local symmetry to monoclinic C_s ($T_C < T < T_S$), releases the orbital degeneracy ($\{d^*_{x^2-y^2}\}$), and deforms the orbitals. The ordering to the ferrimagnetic magnetic state ($T < T_C$) further distorts the orbitals and selects only one (d^{**}). Temperature dependence of the (b) and (c) pyroelectric polarization and (d)–(g) dielectric constant of $CaBaCo_4O_7$ and $CaBaFe_2Co_2O_7$, respectively. The (h) inset shows the peak in the imaginary part of $\epsilon_{\parallel z}$ at T_C.

the damping rate have been detected in emblematic multiferroics including manganites $RMnO_3$ (R = Ho, Y) [61,62], $TbMnO_3$ [63], RMn_2O_5 (R = Tb, Eu, Dy, Bi) [64,65], delafossite $CuFeO_2$ [66], or $Ni_3V_2O_8$ [67]. Although several

different mechanisms are responsible for the spin-lattice coupling in these materials, ranging from exchange striction [11,68], inverse Dzyaloshinskii-Moriya interaction [8,9] to on site anisotropy term [12], none of them results in such a strong magnetic-order-induced change of phonon lifetime. We note that charge fluctuations are frozen in the studied Swedenborgites as indicated by the large dc resistivity and the corresponding few-100 meV optical charge gap (see Figs. S2 and S7 in the Supplemental Material [24]); thus, these cannot modify the spin-lattice interaction. Instead, we argue that low-energy fluctuations of the orbital degrees of freedom open a new channel and mediate a more efficient spin-lattice interaction in $CaBaCo_4O_7$ and $CaBaFe_4O_7$ since orbitals can strongly interact with both spin fluctuations and phonons. This may lead to considerable broadening of phonon modes when the ordered state becomes paramagnetic as demonstrated in $LaTiO_3$ [46]. It is instructive to compare the case of Swedenborgites to that of hexagonal manganites. Although both classes of compounds crystallize in a polar structure with geometric frustration, the phonons are scattered strongly by spin fluctuations exclusively in the Swedenborgites. In hexagonal mangnites, Mn^{3+} ions sit in a trigonal bipyramid; thus, they have $S = 2$ spins just like tetrahedrally coordinated Co^{3+} and Fe^{2+} ions. However, they are not Jahn-Teller active, and their orbital singlet ground state is well separated from other 3d states [69,70]. This fact also suggests that the presence of orbital degrees of freedom allows the unusually strong spin-lattice coupling in Swedenborgites. Finally, we mention that a recent study of infrared phonons in $Fe_2Mo_3O_8$ shows similar enhancement of the damping rate across its antiferromagnetic phase transition [44].

In $CaBaCo_4O_7$ and $CaBaFe_4O_7$, both the tetrahedrally coordinated Co^{3+} and Fe^{2+} ions possess the orbital-degenerate ^5E ground state multiplet as shown in the inset of Fig. 2. The orbital degeneracy is released by the trigonal to orthorhombic phase transition at T_S, as illustrated in Fig. 4(a). The symmetry of the surrounding oxygen ligands is reduced to monoclinic, the $d_{x^2-y^2}$ and d_{xy} orbitals are separated by a small energy gap, and mixed with $d_{3z^2-r^2}$ orbitals [27,29]. Since these strongly fluctuating low-symmetry orbitals can efficiently couple to the lattice, the phonons strongly scatter on this hybridized ground state in the paramagnetic phase. As the magnetic order develops, the second-order spin-orbit interaction can further polarize the orbitals; as an example spins along the y axis favor the $d_{z^2-x^2}$ orbital [71,72]. The magnetic order in $CaBaCo_4O_7$ selects the same orbital shape at each Co^{3+} site and consequently reduces the fluctuations. According to this scenario, the quenching of the orbitals at T_C strongly influences the lattice as well [23], which explains the exceptionally large magnetostriction, magnetic-order-induced polarization, and change in the dielectric response in $CaBaCo_4O_7$ and $CaBaFe_4O_7$. The on site anisotropy as well as the orbital dependence of the exchange interactions (Kugel-Khomskiĭ-type interaction) may equally play an important role in the enhanced spin-phonon coupling; however, our experiment is sensitive only to the Γ-point lattice vibrations. Thus it cannot distinguish between these mechanisms. On one hand, the orbitals may affect the bond orientation dependence of the exchange and its bond-length variation. On the other hand, they may distort the local environment, and spins drive a distortion of the local coordination. This question may be addressed by studying the momentum dependence of the phonon dispersion and lifetime in a scattering experiment. As the magnetic ions in $CaBaFe_2Co_2O_7$ have exclusively orbital-singlet ground states, the magnetic order has no effect on the orbitals, and the absence of orbital degrees of freedom diminishes the spin-lattice coupling. Furthermore, orbital degeneracy can be the driving force behind the phonon anomalies in $Fe_2Mo_3O_8$ [44], as it contains tetrahedrally coordinated Fe^{2+} ions with orbital degrees of freedom, which suggests that the orbitals can enhance magnetoelastic and magnetoelectric couplings not only in Swedenborgites, but also in broader classes of multiferroics. This idea is further supported by the effect of Ni doping in $CaBaCo_4O_7$, where the substitution of orbital singlet Co^{2+} to Ni^{2+} ions with orbital degeneracy leads to further enhancement of the ME effect [73]. Although a precise theoretical description of these materials is challenging, we believe these findings will motivate further experimental and theoretical research.

The authors are grateful to Karlo Penc for fruitful discussions, and to Akiko Kikkawa and Markus Kriener for their technical assistance. V. K. was supported by the Alexander von Humboldt Foundation. This work was supported by the Hungarian National Research, Development and Innovation Office—NKFIH Grant No. FK 135003 and the bilateral program of the Estonian and Hungarian Academies of Sciences under Contract No. NKM 2021-24, and by the Estonian Research Council Grant No. PRG736, institutional research funding IUT23-3 of the Estonian Ministry of Education and Research and the European Regional Development Fund Project No. TK134. Illustration of the structural unit cell was created using the software VESTA [74].

[1] M. Z. Hasan and C. L. Kane, Rev. Mod. Phys. **82**, 3045 (2010).
[2] X.-L. Qi and S.-C. Zhang, Rev. Mod. Phys. **83**, 1057 (2011).
[3] Z. K. Liu, B. Zhou, Y. Zhang, Z. J. Wang, H. M. Weng, D. Prabhakaran, S.-K. Mo, Z. X. Shen, Z. Fang, X. Dai, Z. Hussain, and Y. L. Chen, Science **343**, 864 (2014).
[4] S.-Y. Xu *et al.*, Science **349**, 613 (2015).
[5] A. Kitaev, Ann. Phys. (Amsterdam) **321**, 2 (2006).
[6] M. Fiebig, J. Phys. D **38**, R123 (2005).
[7] Y. Tokura, S. Seki, and N. Nagaosa, Rep. Prog. Phys. **77**, 076501 (2014).

[8] H. Katsura, N. Nagaosa, and A. V. Balatsky, Phys. Rev. Lett. **95**, 057205 (2005).
[9] I. A. Sergienko and E. Dagotto, Phys. Rev. B **73**, 094434 (2006).
[10] C. Jia, S. Onoda, N. Nagaosa, and J. H. Han, Phys. Rev. B **74**, 224444 (2006).
[11] C. Jia, S. Onoda, N. Nagaosa, and J. H. Han, Phys. Rev. B **76**, 144424 (2007).
[12] T. Arima, J. Phys. Soc. Jpn. **76**, 073702 (2007).
[13] K. I. Kugel' and D. I. Khomskiĭ, Sov. Phys. Usp. **25**, 231 (1982).
[14] Y. Tokura and N. Nagaosa, Science **288**, 462 (2000).
[15] J. van den Brink and D. I. Khomskii, J. Phys. Condens. Matter **20**, 434217 (2008).
[16] K. Yamauchi and S. Picozzi, Phys. Rev. B **85**, 085131 (2012).
[17] G. T. Rado and J. M. Ferrari, Phys. Rev. B **12**, 5166 (1975).
[18] K. Kato and S. Iida, J. Phys. Soc. Jpn. **51**, 1335 (1982).
[19] M. Alexe, M. Ziese, D. Hesse, P. Esquinazi, K. Yamauchi, T. Fukushima, S. Picozzi, and U. Gösele, Adv. Mater. **21**, 4452 (2009).
[20] J. de Groot, T. Mueller, R. A. Rosenberg, D. J. Keavney, Z. Islam, J.-W. Kim, and M. Angst, Phys. Rev. Lett. **108**, 187601 (2012).
[21] R. D. Johnson, L. C. Chapon, D. D. Khalyavin, P. Manuel, P. G. Radaelli, and C. Martin, Phys. Rev. Lett. **108**, 067201 (2012).
[22] N. Perks, R. Johnson, C. Martin, L. Chapon, and P. Radaelli, Nat. Commun. **3**, 1277 (2012).
[23] V. Caignaert, V. Pralong, V. Hardy, C. Ritter, and B. Raveau, Phys. Rev. B **81**, 094417 (2010).
[24] See Supplemental Material at http://link.aps.org/supplemental/10.1103/PhysRevLett.130.036801 for additional specific heat, reflectivity, and dielectric constant measurements, which includes Refs. [25,26].
[25] P. Lunkenheimer, V. Bobnar, A. V. Pronin, A. I. Ritus, A. A. Volkov, and A. Loidl, Phys. Rev. B **66**, 052105 (2002).
[26] P. Lunkenheimer, S. Krohns, S. Riegg, S. Ebbinghaus, A. Reller, and A. Loidl, Eur. Phys. J. Special Topics **180**, 61 (2009).
[27] N. Hollmann, Z. Hu, H. Wu, M. Valldor, N. Qureshi, T. Willers, Y.-Y. Chin, J. C. Cezar, A. Tanaka, N. B. Brookes, and L. H. Tjeng, Phys. Rev. B **83**, 180405(R) (2011).
[28] V. Kocsis, Y. Tokunaga, S. Bordács, M. Kriener, A. Puri, U. Zeitler, Y. Taguchi, Y. Tokura, and I. Kézsmárki, Phys. Rev. B **93**, 014444 (2016).
[29] S. Chatterjee and T. Saha-Dasgupta, Phys. Rev. B **84**, 085116 (2011).
[30] V. Cuartero, J. Blasco, G. Subías, J. García, J. A. Rodríguez-Velamazán, and C. Ritter, Inorg. Chem. **57**, 3360 (2018).
[31] V. R. Galakhov, S. N. Shamin, and V. V. Mesilov, JETP Lett. **107**, 583 (2018).
[32] J. D. Reim, E. Rosén, W. Schweika, M. Meven, N. R. Leo, D. Meier, M. Fiebig, M. Schmidt, C.-Y. Kuo, T.-W. Pi, Z. Hu, and M. Valldor, J. Appl. Crystallogr. **47**, 2038 (2014).
[33] T. Omi, Y. Watanabe, N. Abe, H. Sagayama, A. Nakao, K. Munakata, Y. Tokunaga, and T.-h. Arima, Phys. Rev. B **103**, 184412 (2021).
[34] S. Bordács, V. Kocsis, Y. Tokunaga, U. Nagel, T. Rõõm, Y. Takahashi, Y. Taguchi, and Y. Tokura, Phys. Rev. B **92**, 214441 (2015).
[35] V. Caignaert, A. Maignan, K. Singh, C. Simon, V. Pralong, B. Raveau, J. F. Mitchell, H. Zheng, A. Huq, and L. C. Chapon, Phys. Rev. B **88**, 174403 (2013).
[36] R. D. Johnson, K. Cao, F. Giustino, and P. G. Radaelli, Phys. Rev. B **90**, 045129 (2014).
[37] Y.-S. Chai, J.-Z. Cong, J.-C. He, D. Su, X.-X. Ding, J. Singleton, V. Zapf, and Y. Sun, Phys. Rev. B **103**, 174433 (2021).
[38] M. Soda, Y. Yasui, T. Moyoshi, M. Sato, N. Igawa, and K. Kakurai, J. Phys. Soc. Jpn. **75**, 054707 (2006).
[39] J. D. Reim, E. Rosén, O. Zaharko, M. Mostovoy, J. Robert, M. Valldor, and W. Schweika, Phys. Rev. B **97**, 144402 (2018).
[40] M. Valldor, N. Hollmann, J. Hemberger, and J. A. Mydosh, Phys. Rev. B **78**, 024408 (2008).
[41] M. Valldor, R. P. Hermann, J. Wuttke, M. Zamponi, and W. Schweika, Phys. Rev. B **84**, 224426 (2011).
[42] J. Laverdière, S. Jandl, A. A. Mukhin, V. Y. Ivanov, V. G. Ivanov, and M. N. Iliev, Phys. Rev. B **73**, 214301 (2006).
[43] R. Basistyy, T. N. Stanislavchuk, A. A. Sirenko, A. P. Litvinchuk, M. Kotelyanskii, G. L. Carr, N. Lee, X. Wang, and S.-W. Cheong, Phys. Rev. B **90**, 024307 (2014).
[44] S. Reschke, A. A. Tsirlin, N. Khan, L. Prodan, V. Tsurkan, I. Kézsmárki, and J. Deisenhofer, Phys. Rev. B **102**, 094307 (2020).
[45] K. Wakamura and T. Arai, J. Appl. Phys. **63**, 5824 (1988).
[46] C. Ulrich, G. Khaliullin, M. Guennou, H. Roth, T. Lorenz, and B. Keimer, Phys. Rev. Lett. **115**, 156403 (2015).
[47] W. Baltensperger and J. S. Helman, Helv. Phys. Acta **41**, 668 (1968).
[48] W. Baltensperger, J. Appl. Phys. **41**, 1052 (1970).
[49] A. B. Souchkov, J. R. Simpson, M. Quijada, H. Ishibashi, N. Hur, J. S. Ahn, S. W. Cheong, A. J. Millis, and H. D. Drew, Phys. Rev. Lett. **91**, 027203 (2003).
[50] C. J. Fennie and K. M. Rabe, Phys. Rev. Lett. **96**, 205505 (2006).
[51] D. D. Dlott, Annu. Rev. Phys. Chem. **37**, 157 (1986).
[52] P. Foggi and V. Schettino, La Rivista del Nuovo Cimento (1978-1999) **15**, 1 (1992).
[53] J. Fujioka, S. Horiuchi, F. Kagawa, and Y. Tokura, Phys. Rev. Lett. **102**, 197601 (2009).
[54] J. Fujioka, S. Horiuchi, N. Kida, R. Shimano, and Y. Tokura, Phys. Rev. B **80**, 125134 (2009).
[55] P. G. Klemens, Phys. Rev. **148**, 845 (1966).
[56] M. Balkanski, R. F. Wallis, and E. Haro, Phys. Rev. B **28**, 1928 (1983).
[57] H. Iwamoto, M. Ehara, M. Akaki, and H. Kuwahara, J. Phys. Conf. Ser. **400**, 032031 (2012).
[58] A. B. Sushkov, R. V. Aguilar, S. Park, S.-W. Cheong, and H. D. Drew, Phys. Rev. Lett. **98**, 027202 (2007).
[59] G. Lawes, A. P. Ramirez, C. M. Varma, and M. A. Subramanian, Phys. Rev. Lett. **91**, 257208 (2003).
[60] G. Lawes, T. Kimura, C. M. Varma, M. A. Subramanian, N. Rogado, R. J. Cava, and A. P. Ramirez, Prog. Solid State Chem. **37**, 40 (2009).
[61] A. P. Litvinchuk, M. N. Iliev, V. N. Popov, and M. M. Gospodinov, J. Phys. Condens. Matter **16**, 809 (2004).

[62] M. Zaghrioui, V. Ta Phuoc, R. A. Souza, and M. Gervais, Phys. Rev. B **78**, 184305 (2008).
[63] R. Schleck, R. L. Moreira, H. Sakata, and R. P. S. M. Lobo, Phys. Rev. B **82**, 144309 (2010).
[64] R. Valdés Aguilar, A. B. Sushkov, S. Park, S.-W. Cheong, and H. D. Drew, Phys. Rev. B **74**, 184404 (2006).
[65] A. F. Garcia-Flores, E. Granado, H. Martinho, R. R. Urbano, C. Rettori, E. I. Golovenchits, V. A. Sanina, S. B. Oseroff, S. Park, and S.-W. Cheong, Phys. Rev. B **73**, 104411 (2006).
[66] O. Aktas, K. D. Truong, T. Otani, G. Balakrishnan, M. J. Clouter, T. Kimura, and G. Quirion, J. Phys. Condens. Matter **24**, 036003 (2011).
[67] L. I. Vergara, J. Cao, N. Rogado, Y. Q. Wang, R. P. Chaudhury, R. J. Cava, B. Lorenz, and J. L. Musfeldt, Phys. Rev. B **80**, 052303 (2009).
[68] M. Matsumoto, K. Chimata, and M. Koga, J. Phys. Soc. Jpn. **86**, 034704 (2017).
[69] C. Degenhardt, M. Fiebig, D. Fröhlich, T. Lottermoser, and R. V. Pisarev, Appl. Phys. B **73**, 139 (2001).
[70] S. Lee, A. Pirogov, M. Kang, K.-H. Jang, M. Yonemura, T. Kamiyama, S.-W. Cheong, F. Gozzo, N. Shin, H. Kimura, Y. Noda, and J.-G. Park, Nature (London) **451**, 805 (2008).
[71] S. Ohtani, Y. Watanabe, M. Saito, N. Abe, K. Taniguchi, H. Sagayama, T. Arima, M. Watanabe, and Y. Noda, J. Phys. Condens. Matter **22**, 176003 (2010).
[72] Y. Nii, H. Sagayama, T. Arima, S. Aoyagi, R. Sakai, S. Maki, E. Nishibori, H. Sawa, K. Sugimoto, H. Ohsumi, and M. Takata, Phys. Rev. B **86**, 125142 (2012).
[73] M. Gen, A. Miyake, H. Yagiuchi, Y. Watanabe, A. Ikeda, Y. H. Matsuda, M. Tokunaga, T. Arima, and Y. Tokunaga, Phys. Rev. B **105**, 214412 (2022).
[74] K. Momma and F. Izumi, J. Appl. Crystallogr. **41**, 653 (2008).